Dipole-dipole interaction between rubidium Rydberg atoms

Emily Altiere,[1] Donald P. Fahey,[1] Michael W. Noel,[1] Rachel J. Smith,[2] and Thomas J. Carroll[2]
[1]*Physics Department, Bryn Mawr College, Bryn Mawr, Pennsylvania 19010, USA*
[2]*Department of Physics and Astronomy, Ursinus College, Collegeville, Pennsylvania 19426, USA*
(Received 10 June 2011; published 28 November 2011)

Ultracold Rydberg atoms in a static electric field can exchange energy via the dipole-dipole interaction. The Stark effect shifts the energy levels of the atoms which tunes the energy exchange into resonance at specific values of the electric field (Förster resonances). We excite rubidium atoms to Rydberg states by focusing either a 480 nm beam from a tunable dye laser or a pair of diode lasers into a magneto-optical trap. The trap lies at the center of a configuration of electrodes. We scan the electric field by controlling the voltage on the electrodes while measuring the fraction of atoms that interact. Dipole-dipole interaction spectra are presented for initially excited rubidium nd states for $n = 31$ to 46 and for four different pairs of initially excited rubidium ns states. We also present the dipole-dipole interaction spectra for individual rubidium $32d$ (j, m_j) fine structure levels that have been selectively excited. The data are compared to calculated spectra.

DOI: 10.1103/PhysRevA.84.053431 PACS number(s): 32.80.Ee, 32.80.Rm, 32.60.+i

I. INTRODUCTION

The dipole-dipole interaction provides a strong coupling between atoms in an ultracold Rydberg gas. This interaction can be tuned into resonance with a small electric field, allowing pairs of atoms separated by tens of microns to exchange energy on a time scale of a few microseconds [1–9]. Ultimately, the strong interaction among cold Rydberg atoms may prove useful for quantum computing [10,11]. The dipole blockade has been observed for an ensemble of cesium Rydberg atoms [12,13] and for two Rydberg atoms [14,15]. Recently, two atoms have been entangled using the Rydberg blockade [16,17]. The potential for constructing a quantum computer with this system is explored in an extensive review by Saffman *et al*. [18]. In addition to mediating the exchange of energy among atoms, the dipole-dipole interaction provides an attraction between atoms that can lead to ionizing collisions, which seed the evolution of the sample into an ultracold plasma [19–22]. Ultracold plasmas present interesting opportunities for studies in the strong-coupling regime where the Coulomb interaction between neighboring particles exceeds their kinetic energies [23].

The interest in long-range dipolar interactions in ultracold gases extends well beyond the Rydberg system described here. Recently, researchers have Bose condensed chromium atoms, which have a magnetic dipole moment of 6 Bohr magnetons [24]. The mechanical effects of the dipole-dipole interaction among these atoms have been directly observed in the expansion of the condensate [25]. Another system receiving considerable attention is an ultracold gas of heteronuclear molecules [26,27]. By applying an external electric field to this system the molecules can be polarized, inducing a sizable dipole moment. The long-range nature of the dipole-dipole interaction in all of these systems has begun to reveal a host of new phenomena that promise to give insight into condensed matter physics, plasma physics, and the atomic physics of ultracold gases.

In this paper we present dipole-dipole interaction spectra for atoms initially excited to a broad range of nd energy levels and pairs of ns energy levels. For rubidium nd atoms there are two sets of energy levels that can be tuned into resonance:

$$nd + nd \rightarrow (n-2)\ \text{manifold} + (n+2)p, \tag{1a}$$
$$nd + nd \rightarrow (n+1)p + (n-1)\ \text{manifold}. \tag{1b}$$

The nd atoms participating in the interaction can be any combination of the five (j, m_j) states. For example, Fig. 1 shows two possible resonances of the type in Eq. (1a). Over this field range there are several hundred possible resonances. The up-arrow in Fig. 1 denotes a transition from a $39d$ state to a $41p$ state while the down-arrow denotes a transition from a $39d$ state to an $n = 37$ manifold state. The interactions of the type in Eq. (1b) typically tune into resonance at electric fields higher than those considered in this work. We will refer to the energy exchange of Eqs. (1a) and (1b) as the dd interaction.

For certain pairs of rubidium ns states, the following energy levels can be tuned into resonance:

$$n_1 s + n_2 s \rightarrow (n_1 - 1)p + (n_2 + 1)p, \tag{2}$$

where n_1 and n_2 are two different principal quantum numbers with $n_1 < n_2$. For example, Fig. 2 shows possible resonances of this type with $n_1 = 34s$ and $n_2 = 46s$. The up-arrow in Fig. 2 denotes a transition from the $46s$ state to the $47p$ state while the down-arrow denotes a transition from the $34s$ state to the $33p$ state. We will refer to the energy exchange of Eq. (2) as the ss' interaction.

II. EXPERIMENT

We begin our experiment by trapping about 10^6 atoms in a magneto-optical trap (MOT). We then excite the cold atoms to the desired Rydberg states using pulsed laser light. A static electric field is present during the excitation to tune the energies of the states into resonance where they can exchange energy. Finally, we field ionize the atoms and measure the final state distribution in order to determine how many atoms have exchanged energy.

We trap ^{85}Rb atoms using a 780 nm diode laser in a standard MOT configuration. The trapping lasers cycle atoms between

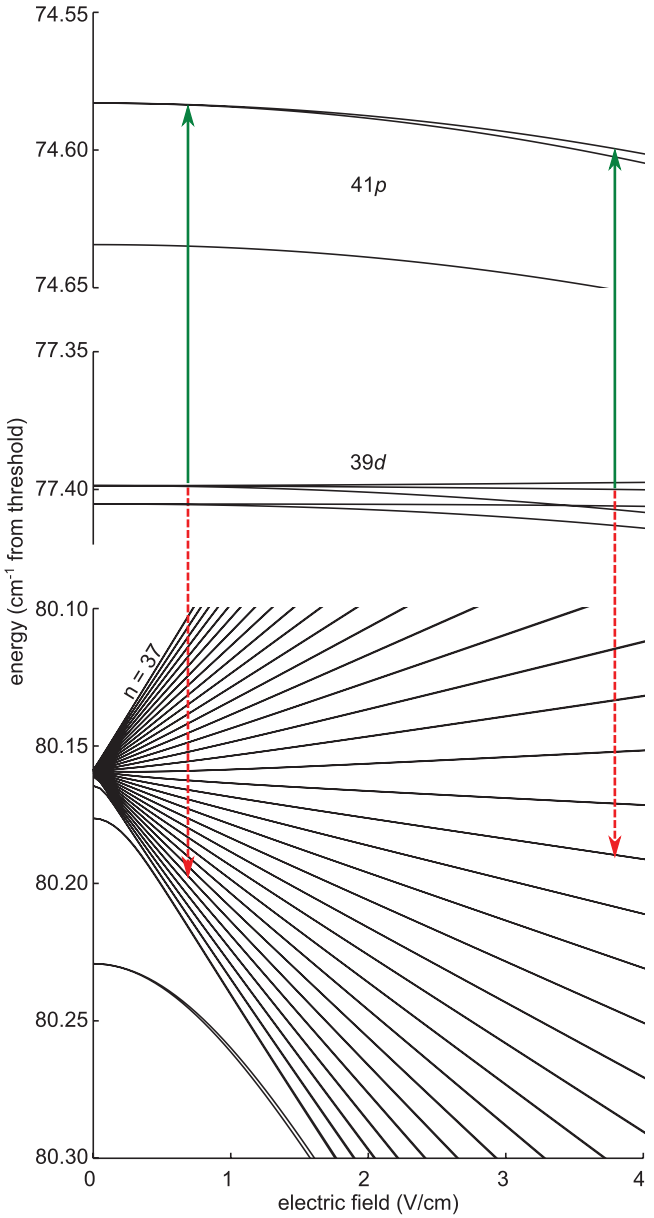

FIG. 1. (Color online) Rb Stark map showing the $n = 37$ manifold, the $39d$ state, and the $41p$ state. For clarity, only the $m_j = 1/2$ states are shown for the manifold. The $37f$ and $37g$ states are visibly separated from the manifold. The up (green, solid) and down (red, dashed) arrows denote the locations of two of the many possible resonant interactions. States in the manifold with a large slope tune into resonance at lower electric fields while "flatter" manifold states tune into resonance at relatively higher electric fields.

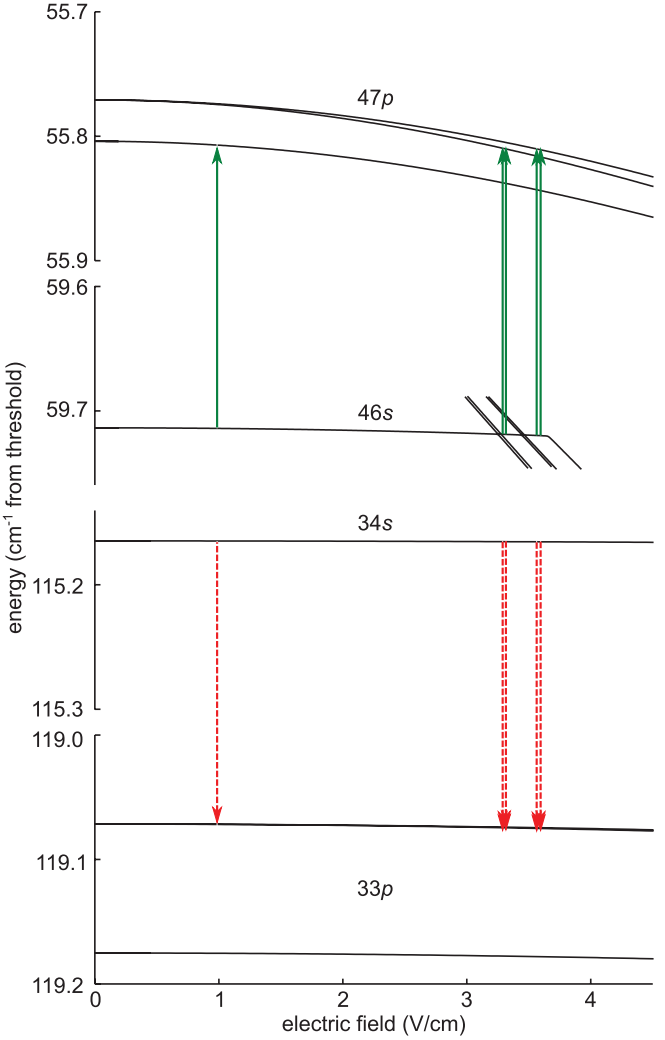

FIG. 2. (Color online) Rb Stark map showing the $33p$, $34s$, $46s$, and $47p$ states. The up (green, solid) and down (red, dashed) arrows denote the locations of resonant interactions.

the $5s_{1/2}$ and $5p_{3/2}$ states. For most of the data presented in this paper, we further excite the atoms from the $5p_{3/2}$ to Rydberg states using a 480 nm neodymium doped, yttrium aluminum garnet (Nd:YAG) pumped dye laser (Coumarin-480). In Figs. 3 and 4 we present dipole-dipole interaction spectra for atoms initially excited to a single nd state. The bandwidth of our dye laser is too broad to resolve the fine structure splitting of the d states so, in practice, our initial state is a mixture of all five (j, m_j) states for a particular nd level.

After excitation, the atoms are allowed to interact for 5 μs in the presence of a static electric field. This field is applied by biasing a pair of cylinders, one on each side of the trapped atoms, at the appropriate voltages. We then scan this field from 0 V/cm to either 2 or 4 V/cm. At various electric fields there are Stark states equally spaced above and below the initial states, which allows pairs of atoms to exchange energy. After the interaction time has concluded, a high-voltage ionization field is applied to the cylinder across from the detector. The field ionizes the initial d state atoms and the higher energy p state atoms resulting from the resonant energy exchange. The ionization pulse causes the freed electrons to accelerate toward the chevron microchannel plate assembly where they are detected. The atoms of energy lower than the initial excited state end up in a manifold state and are not detected. Integrating the time-resolved signal received from atoms in the higher p state scanned over many shots of the laser, we graph the dipole-dipole interaction spectrum. Figures 3 and 4 show the number of atoms that are excited to the upper p state as a function of electric field (V/cm) for the dd interactions from $31d$ to $46d$.

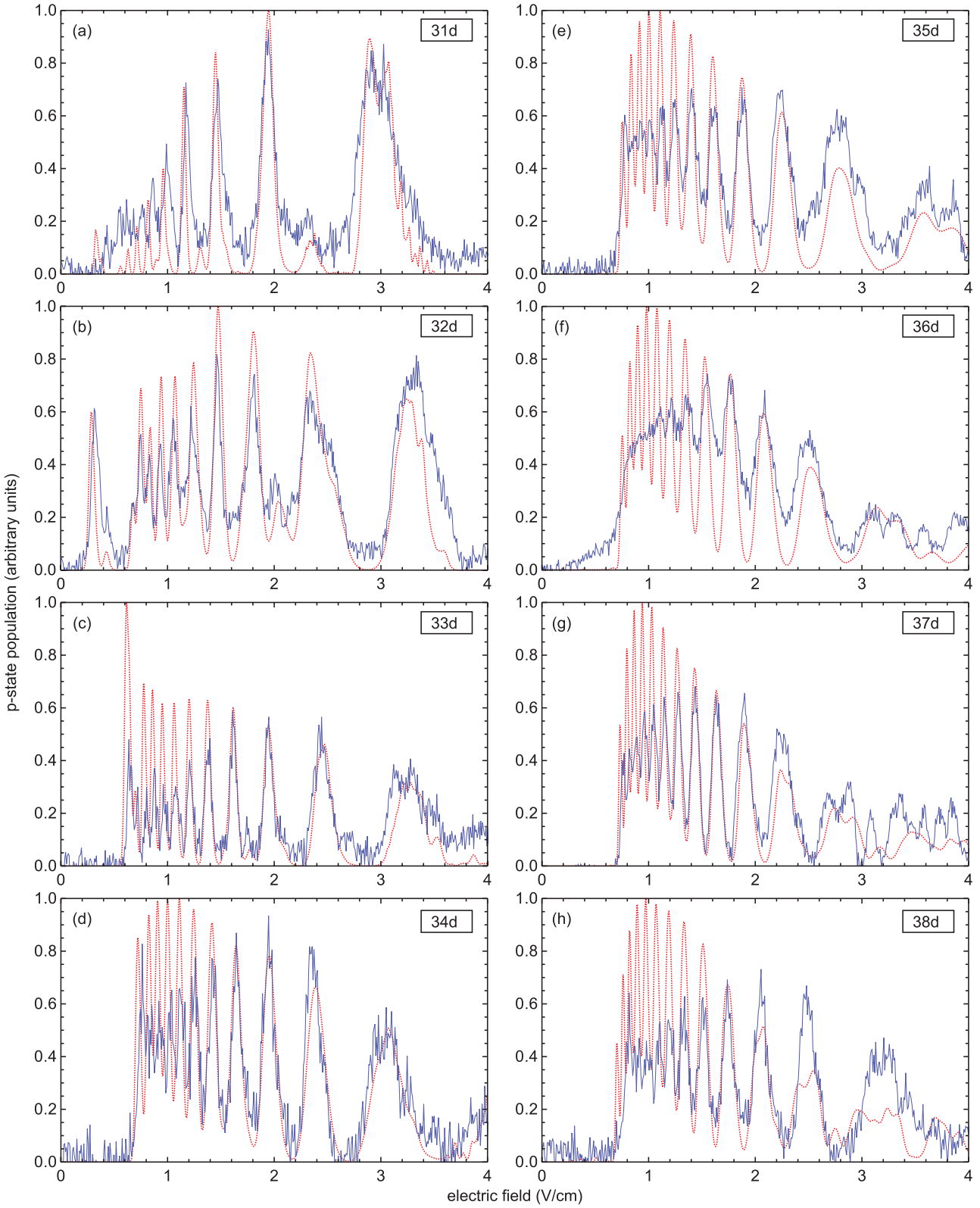

FIG. 3. (Color online) Data (solid blue) and calculation (dashed red) for the dd interactions from 31d to 38d. The 32d spectrum (b) displays a prominent peak at low field that is due to the 30g state.

We have also measured the dipole-dipole interaction spectra for several pairs of initially excited s states (Fig. 5). In this case the experimental procedure is identical except that we use two dye lasers to excite the two s states.

Finally, we have produced high-resolution spectra for the 32d state in which we completely resolve the fine structure splitting in the initial excitation (Fig. 6). This is done by replacing the dye laser with a pair of diode lasers [28]. One

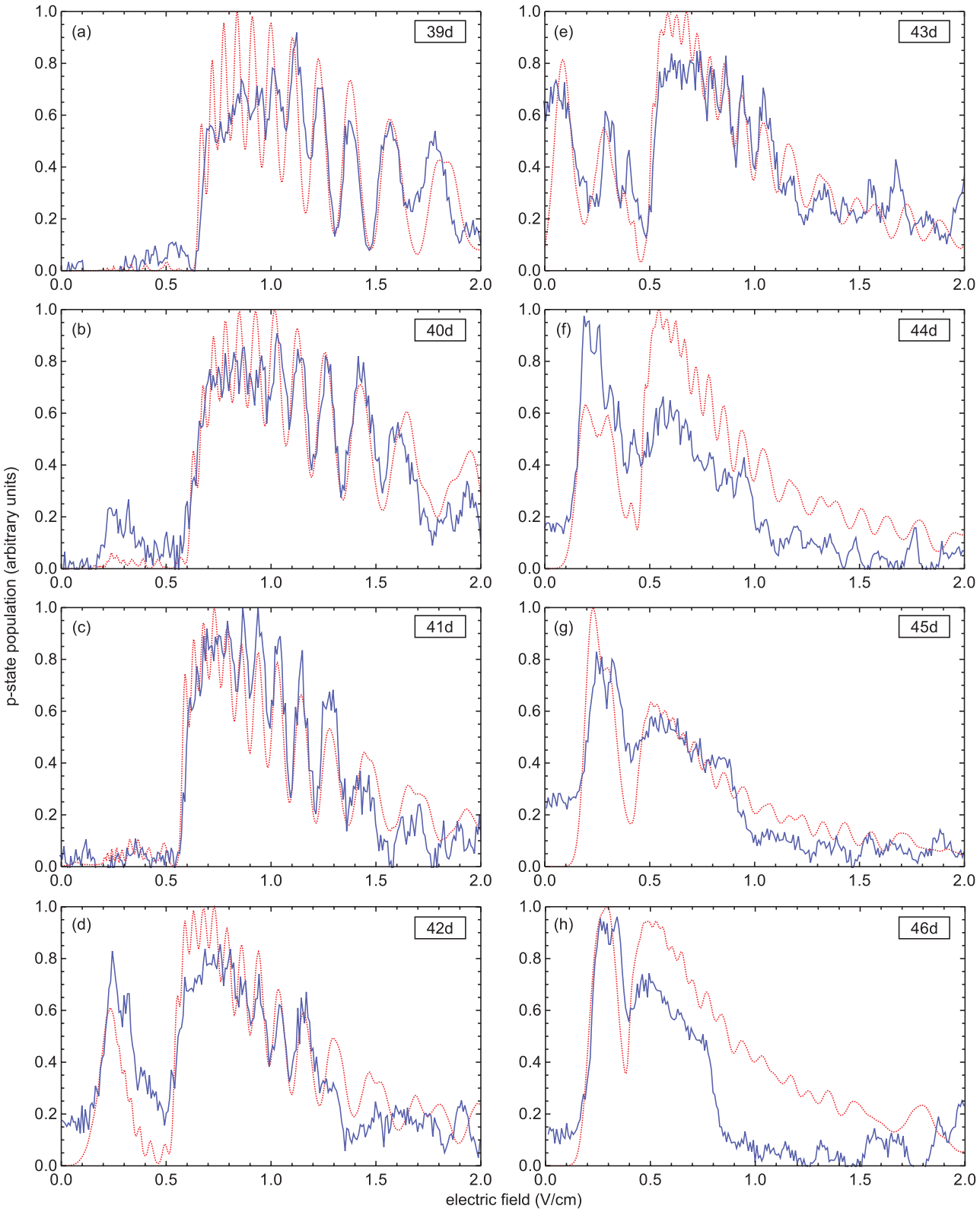

FIG. 4. (Color online) Data (solid blue) and calculation (dashed red) for the dd interactions from 39d to 46d. Many of these states display prominent early peaks that are due to the manifold f and g states.

of the diode lasers drives the $5p \rightarrow 5d$ transition at 776 nm. From the $5d$ state the atoms fluoresce down to the $6p$ state. The final transition to Rydberg levels is from the $6p$ state with laser light near 1022 nm. The narrow bandwidth of these lasers allows us to selectively excite one of the (j, m_j) states, which are split in the presence of a static field as seen in Fig. 1 for the

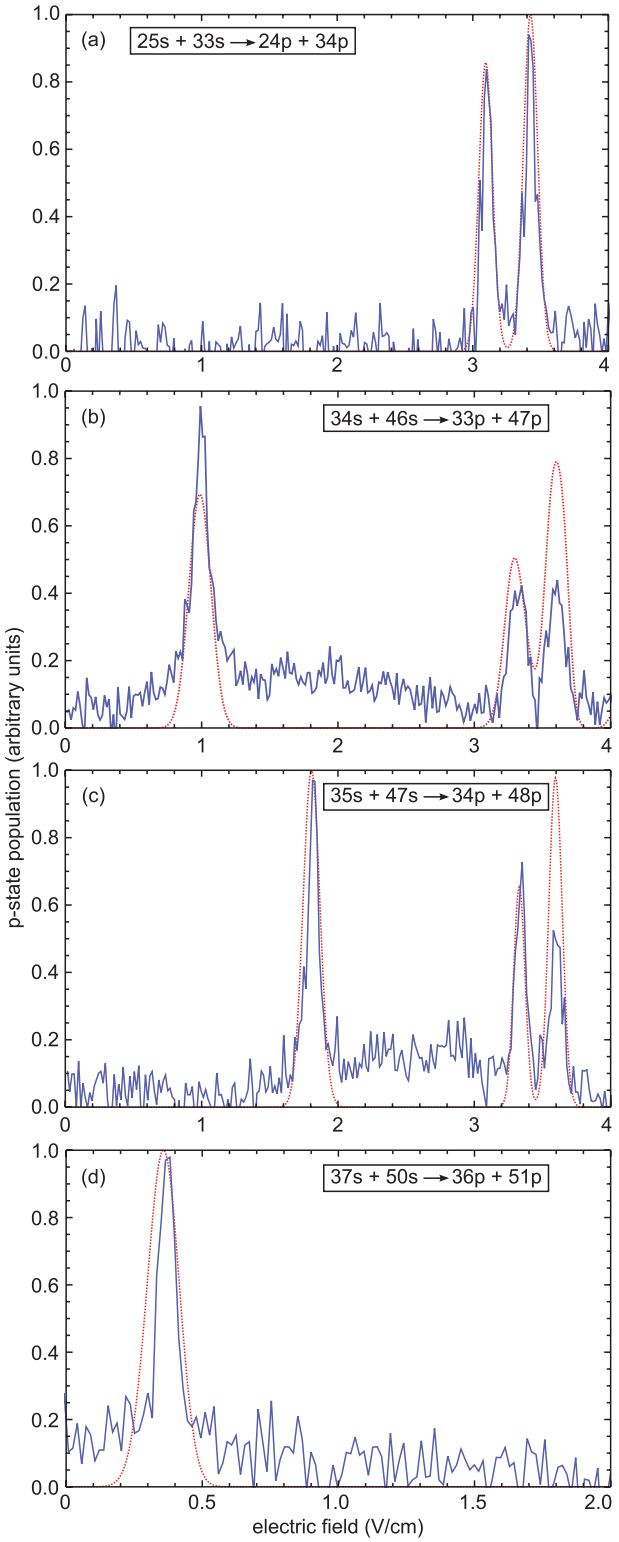

FIG. 5. (Color online) Data (solid blue) and calculation (dashed red) for four different ss' interactions: (a) $25s + 33s \rightarrow 24p + 34p$, (b) $34s + 46s \rightarrow 33p + 47p$, (c) $35s + 47s \rightarrow 34p + 48p$, and (d) $37s + 50s \rightarrow 36p + 51p$.

$39d$ state. We therefore excite the desired state in a 6 V/cm field. Immediately after excitation, the field is switched in less that 200 ns to the "interaction field," which is varied as before to collect spectra.

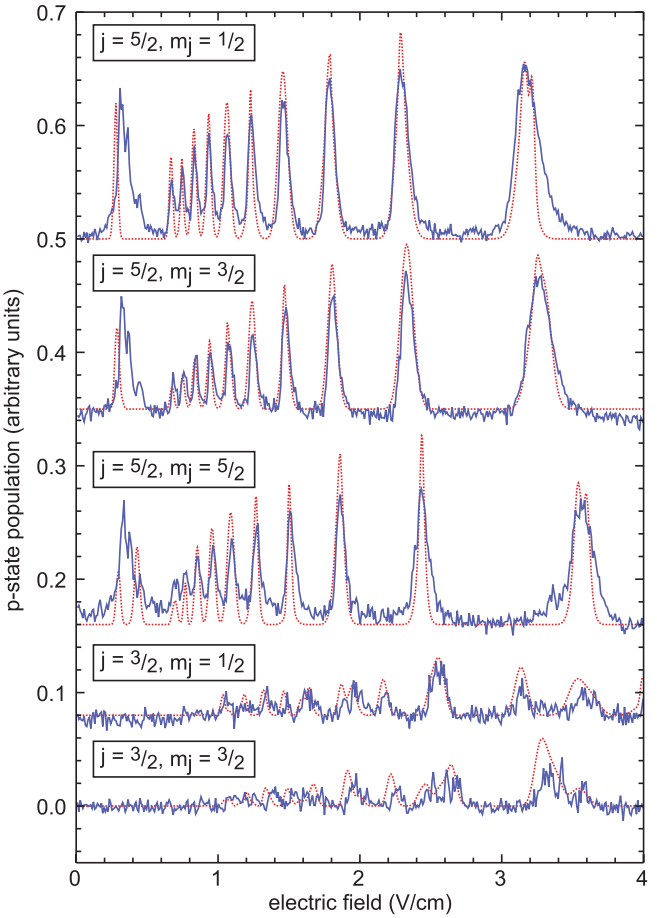

FIG. 6. (Color online) Data (solid blue) and calculation (dashed red) for the dd interactions for individual $32d$ (j, m_j) states. The five spectra are graphed at arbitrary vertical positions for clarity of viewing. The calculations generally agree with the data with the exception of the initial $30g$ peak in the $32d_{5/2}$ states.

III. RESULTS AND DISCUSSION

We have developed a model of the dipole-dipole interaction spectra. The first step is to find all of the dipole-dipole resonances for each dd or ss' interaction. To do so, we created a Stark map at.05 V/cm resolution for the region 0–10 V/cm and $n = 20$ to 60. For each interaction, we search the Stark map for all possible resonances: pairs of initial and final states that satisfy energy conservation and selection rules. For the ss' interactions, there are typically fewer than 10 possible resonances. For the dd interactions, the number of possible resonances for electric fields less than about 4 V/cm ranges from a few hundred at $n = 31$ to a few thousand at $n = 46$.

At the electric field of each possible resonance we calculate the eigenvectors for each initial and final state involved. We use the eigenvectors to calculate the transition dipole moments for each possible resonance (averaging over all atomic orientations). The s, p, and d states are relatively flat in the region of electric field that we examine. These eigenvectors will therefore mostly retain their zero-field character (for convenience we will continue to label the states with their zero-field character). Thus the $d \rightarrow p$ and $s \rightarrow p$ transition dipole moments are relatively large, with typical values of a

few 100 ea_0 for our resonances. Except for the f state, the d state does not couple to the manifold at zero electric field. The manifold states, however, mix significantly as the electric field increases and the $d \rightarrow$ manifold state transition dipole moments become nonzero with typical values of 10 to 20 ea_0.

We estimate the amplitude and width of each resonance by simulating the many-body energy exchange for a range of dipole moments, detunings, and numbers of atoms. We model the dd interaction as a three-level system with an upper p state, an initial d state, and a lower manifold state. We assume that the atoms are initially in the state $|dddd\ldots\rangle$ and we calculate the time evolution.

The simulation is performed by diagonalization of the full dipole-dipole Hamiltonian matrix $\hat{H}$, similar to [29,30]. The off-diagonal elements of the Hamiltonian in atomic units are given by

$$\hat{H}_{k\ell} = \sum_{i \neq j} \hat{\rho}^i_{dp} \hat{\rho}^j_{dm} \frac{\mu\nu}{R^3_{ij}} + \hat{\rho}^i_{dp} \hat{\rho}^j_{pd} \frac{\mu^2}{R^3_{ij}} + \hat{\rho}^i_{dm} \hat{\rho}^j_{md} \frac{\nu^2}{R^3_{ij}}, \quad (3)$$

where k and ℓ refer to different states, i and j refer to individual atoms within each state, and the sum is over all atoms in each state. The operators $\hat{\rho}_{ab}$ take an individual atom from state a to state b, where a and b are the states involved in the dd interaction as shown, for example, in Fig. 1. We ignore any orientation or spin effects and approximate the dipole-dipole interaction coupling by $\mu\nu/R^3_{ij}$ where R_{ij} is the distance between the two atoms. The first term in Eq. (3) is the field-tuned interaction and the next two terms are always resonant interactions. The diagonal elements of the Hamiltonian are given by

$$\hat{H}_{kk} = \sum_{i=j} \hat{\rho}^i_{mm} \Delta/2 + \hat{\rho}^i_{pp} \Delta/2, \quad (4)$$

where the detuning, or energy defect, $\Delta = 2E_d - (E_p + E_m)$. The Hamiltonian for the ss' interaction is similar and is given in [31]. While it has been found that dipole-dipole interactions can lead to consequential atomic motion [19,32], we assume that we are in the regime of a "frozen gas." We therefore assume that the atoms are stationary on the time scales and densities studied. We also simplify the calculation by treating the dipole-dipole interaction as a process that occurs after the excitation of the atoms to Rydberg states, with no overlap in time.

We simulate the interactions by randomly placing some number of Rydberg atoms in a cylindrical volume. Most of our results for the dd interaction are for 9-atom simulations where it is easy for us to generate good statistics since the 3139×3139 Hamiltonian matrix can be diagonalized efficiently. Similarly, most of our results for the ss' interaction are for 12 total atoms where the Hamiltonian matrix is a maximum of 924×924. The exact size of the ss' Hamiltonian depends on the specific mixture of s and s' atoms. For our simulations, we averaged over all possible combinations of s and s' atoms yielding 12 total atoms. In the case of 9 atoms, the cylindrical region is 164 μm long with a 20 μm radius. We keep the density fixed for other numbers of atoms by fixing the diameter and changing the length of the line.

In the experiment, we do not attempt to measure the number of Rydberg atoms excited. The dd resonances for the states we examined are closely spaced: within the width of one resonance there are likely to be multiple additional resonances with comparable dipole moments. For the data presented in Figs. 3 and 4, we are also exciting a mixture of initial $d\,(j, m_j)$ sublevels of which different combinations may participate in each resonance. In fact, for some combinations of resonances, individual atoms may be able to simultaneously participate in multiple resonances (a possibility that our simulation ignores). For these reasons it is difficult to measure how many atoms are participating in each resonance. Our approach instead is to simulate the peak widths for various numbers of Rydberg atoms to establish a range for the spectral fits.

Figure 7 shows some results of these simulations for the dd and ss' interactions. Figure 7(a) shows the peak width as a function of the dipole-dipole interaction coupling strength (represented by the product of the dipole moments) for the dd interaction with 9 total atoms (blue circles) and for the ss' interaction for 12 total atoms (red squares). The peak width increases linearly with the product of the dipole moments in both cases, although the slope is significantly smaller for the ss' case. Examples of simulated peaks for a range of atom numbers at fixed density and fixed dipole moment for the dd interaction are shown in Fig. 7(c), where we plot an adjusted fraction of atoms excited to the p state vs detuning. We find that, as the number of atoms is increased, the fraction of atoms excited to the p state also increases. In Fig. 7(c) we have adjusted this amplitude so that the peak widths can be more directly compared. As is evident in Fig. 7(c) the peak widths converge as we include 9 to 11 atoms in our simulation. For 5 to 9 atoms, we averaged 1000 or more runs of the simulation at each of 20 detunings. At 10 atoms we averaged 500 runs. Our simulations were limited to 11 atoms where we averaged only 100 runs (since the Hamiltonian matrix is $256\,53 \times 256\,53$ the 11-atom case is significantly more computationally intensive).

The widths of the peaks are determined partly by the many-body nature of the interaction and the electric field inhomogeneity. The electric field inhomogeneity should be approximately the same for all interactions studied and is modeled as a free parameter that is adjusted to achieve a better fit to the data. The range of field inhomogeneities used in fitting the data is consistent with an estimate of a residual field variation of $\sim$1% over the volume of Rydberg atoms, made by modeling our interaction region using the software package SIMION. Based on the simulation data in Fig. 7, we calculate the many-body component of the width of each resonance by multiplying the product of the dipole moments by a constant. The constant is chosen to best fit the data but is similar in magnitude to the slopes of the best fit lines in Fig. 7(a). To convert the many-body width from atomic units to V/cm we determine the slope of each resonance. The manifold states involved in a resonance primarily determine this slope. Figure 1 shows two possible resonances: one at a lower field near 1 V/cm and one at a higher field near 4 V/cm. At lower fields, low ℓ manifold states with a high slope tune into resonance first. At higher fields, states closer to the middle of the manifold with smaller slopes tune into resonance. This will cause resonances at higher fields to be broader compared to resonances at lower fields. This effect is observed in the data; for example, see Fig. 3(d) which shows

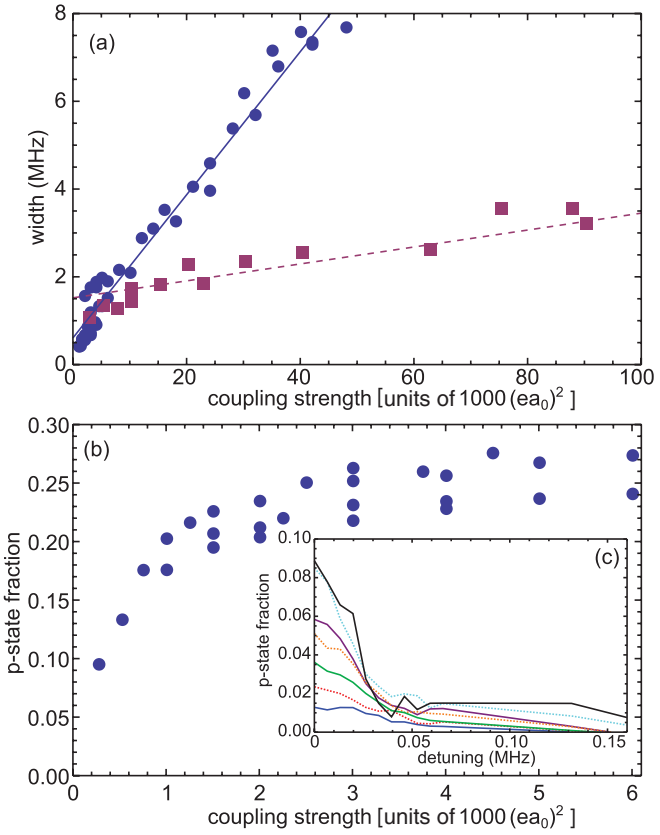

FIG. 7. (Color online) Various components of the model used to calculate the dipole-dipole spectra shown in Figs. 3, 4, and 5. (a) Peak widths were simulated for the dd interaction (blue circles) and the ss' interaction (red squares) at a variety of coupling strengths (product of the transition dipole moments). In both cases the simulated data fit well to a linear model. For the same atomic density and coupling strength, the dd interaction (solid blue line) has a larger width than the ss' interaction (dashed red line). (b) The time-averaged fraction of atoms excited to the p state is shown for the dd interaction as a function of coupling strength. This plot was generated by simulating 9 atoms at fixed density. For a wide range of coupling strengths the fraction of atoms excited to the p state saturates. (c) Sample simulated peaks for the dd interaction. Atoms were simulated at fixed density in a cylindrical volume. The shortest peak (solid blue) is the result of a 5-atom simulation. Progressively taller peaks are the results of simulations including 6, 7, 8, 9, 10, and 11 atoms. The amplitudes of the peaks have been adjusted so that the peak widths can be more directly compared.

the d-state interaction for the $34d$ state. An exception to this trend can be seen in Fig. 3(b) and Figs. 4(d)–4(h), all of which exhibit a relatively broad peak at low field [33]. These peaks are due to the relatively flat (at low field) f and g states, which are slightly displaced from the manifold due to their small quantum defects.

Comparing Figs. 3 and 4 to Fig. 5, one can see that the experimental peak widths for the dd and ss' interactions are of similar order of magnitude. The simulations predict that the many-body width for the ss' interaction increases more slowly with coupling strength than for the dd interaction, but there are two effects which act to broaden the ss' peaks. First, the s and p states involved in the ss' interaction are all relatively flat in electric field compared to the manifold states involved in the dd interaction. Second, the product of the dipole moments is larger for the ss' interaction because both transition dipole moments are on the order of a few 100 ea_0.

Another potential source of broadening of the dipole-dipole interaction resonances is the presence of ions. The interaction between atoms produces a mechanical force that, in the attractive case, can cause them to collide and ionize [19,34]. We do not see ions present in our field ionization signal and therefore neglect this as a potential source of broadening in our calculations.

We use a simple model for the peak amplitudes. In Fig. 7(b) we graph the fraction of atoms excited to the p state as a function of the dipole-dipole coupling strength for the dd interaction. These simulation results indicate that the fraction of atoms excited to the upper p state increases with time to a steady state saturation value that is similar for a wide range of dipole moments. Figure 7(b) shows that this saturation value is about 0.25 for the dd interaction (when simulating 9 atoms). For smaller dipole moments the fraction of atoms excited to the p state drops rapidly to zero. In our model we assume that, below some cutoff value of the coupling strength, the fraction of atoms excited to the p state drops linearly to zero. Above this cutoff value the fraction of atoms excited to the p state is constant. The cutoff value is chosen to achieve a good fit to the data.

We evaluate the model by independently fitting each data set to the corresponding calculated spectrum. We use a standard χ^2 minimization with four free parameters. Two of the parameters are simply used to subtract background and adjust the vertical scale of the data to match the calculations. The other two parameters determine the horizontal offset and the horizontal scale. The horizontal offset and the horizontal scale should be the same for all spectra, with small variations caused by the MOT location or the pointing of the Rydberg excitation beam, both of which determine the region of electric field that is sampled. We calculate a horizontal offset of $-.01 \pm .01$ V/cm, consistent with zero experimental offset. The horizontal scale is determined to be 0.0082 ± 0.0001 V/cm per data point. The standard deviation of $<2\%$ over a broad range of interactions is indicative of the success of our model.

We have also modeled the dd interaction spectra for the $32d$ state where we have excited individual (j, m_j) states, which is shown in Fig. 6. Each spectrum should involve only interactions between identical $32d$ atoms. For that reason the spectra in Fig. 6 should not sum to the $32d$ spectrum in Fig. 3(b) because any resonances that involve pairs of $32d$ atoms in different fine structure states are excluded. At higher fields the model spectra match quite well with the data. However, for the low-field $30g$ peak, there is poor agreement between the model and the data. In fact, the initial peak looks quite similar for all three of the $j = 5/2$ states. One possible reason for this discrepancy is that our model oversimplifies the energy exchange among the atoms. There are many resonances within the initial peak that are spaced so closely that the atoms could participate in multiple resonances. We plan further experiments to explore the effect of this more complex energy level structure.

IV. CONCLUSION

We have observed dipole-dipole interaction spectra for ultracold atoms excited to a broad range of Rydberg states. For atoms initially excited to nd states, a complicated spectrum of resonances is seen as the electric field is varied. In spite of this complexity, our model does a good job of reproducing the widths and locations of the resonances. Using narrow bandwidth excitation of the $32d$ Rydberg state, we demonstrate the ability to selectively excite a particular (j, m_j) state, which significantly reduces the number of possible resonances for energy exchange. In contrast, the energy exchange between an ss' pair is much simpler. In addition to the $25s + 33s$ spectrum, which was the subject of one of the first studies of resonant energy exchange among ultracold Rydberg atoms [1], we have identified several other ss' pairs that exhibit low field resonances. These may be useful in studies where the initial distribution of atoms is spatially localized [7,31].

ACKNOWLEDGMENTS

This work was based upon work supported by the National Science Foundation under Grant No. 0653544. This work used the Extreme Science and Engineering Discovery Environment (XSEDE), which is supported by National Science Foundation Grant No. OCI-1053575.

[1] W. R. Anderson, J. R. Veale, and T. F. Gallagher, Phys. Rev. Lett. **80**, 249 (1998).
[2] I. Mourachko, D. Comparat, F. de Tomasi, A. Fioretti, P. Nosbaum, V. M. Akulin, and P. Pillet, Phys. Rev. Lett. **80**, 253 (1998).
[3] A. Fioretti, D. Comparat, C. Drag, T. F. Gallagher, and P. Pillet, Phys. Rev. Lett. **82**, 1839 (1999).
[4] W. R. Anderson, M. P. Robinson, J. D. D. Martin, and T. F. Gallagher, Phys. Rev. A **65**, 063404 (2002).
[5] I. Mourachko, W. Li, and T. F. Gallagher, Phys. Rev. A **70**, 031401 (2004).
[6] K. Afrousheh, P. Bohlouli-Zanjani, D. Vagale, A. Mugford, M. Fedorov, and J. D. D. Martin, Phys. Rev. Lett. **93**, 233001 (2004).
[7] C. S. E. van Ditzhuijzen, A. F. Koenderink, J. V. Hernández, F. Robicheaux, L. D. Noordam, and H. B. van Linden van den Heuvell, Phys. Rev. Lett. **100**, 243201 (2008).
[8] T. F. Gallagher and P. Pillet, in *Advances in Atomic, Molecular, and Optical Physics*, edited by Ennio Arimondo *et al.*, Vol. 56 (Academic Press, London, 2008), pp. 161–218.
[9] N. Saquet, A. Cournol, J. Beugnon, J. Robert, P. Pillet, and N. Vanhaecke, Phys. Rev. Lett. **104**, 133003 (2010).
[10] D. Jaksch, J. I. Cirac, P. Zoller, S. L. Rolston, R. Côté, and M. D. Lukin, Phys. Rev. Lett. **85**, 2208 (2000).
[11] M. D. Lukin, M. Fleischhauer, R. Cote, L. M. Duan, D. Jaksch, J. I. Cirac, and P. Zoller, Phys. Rev. Lett. **87**, 037901 (2001).
[12] T. Vogt, M. Viteau, J. Zhao, A. Chotia, D. Comparat, and P. Pillet, Phys. Rev. Lett. **97**, 083003 (2006).
[13] T. Vogt, M. Viteau, A. Chotia, J. Zhao, D. Comparat, and P. Pillet, Phys. Rev. Lett. **99**, 073002 (2007).
[14] A. Gaëtan, Y. Miroshnychenko, T. Wilk, A. Chotia, M. Viteau, D. Comparat, P. Pillet, A. Browaeys, and P. Grangier, Nature Phys. **5**, 115 (2009).
[15] E. Urban, T. A. Johnson, T. Henage, L. Isenhower, D. D. Yavuz, T. G. Walker, and M. Saffman, Nature Phys. **5**, 110 (2009).
[16] T. Wilk, A. Gaëtan, C. Evellin, J. Wolters, Y. Miroshnychenko, P. Grangier, and A. Browaeys, Phys. Rev. Lett. **104**, 010502 (2010).
[17] L. Isenhower, E. Urban, X. L. Zhang, A. T. Gill, T. Henage, T. A. Johnson, T. G. Walker, and M. Saffman, Phys. Rev. Lett. **104**, 010503 (2010).
[18] M. Saffman, T. G. Walker, and K. Mølmer, Rev. Mod. Phys. **82**, 2313 (2010).
[19] W. Li, P. J. Tanner, and T. F. Gallagher, Phys. Rev. Lett. **94**, 173001 (2005).
[20] M. P. Robinson, B. Laburthe Tolra, M. W. Noel, T. F. Gallagher, and P. Pillet, Phys. Rev. Lett. **85**, 4466 (2000).
[21] S. K. Dutta, D. Feldbaum, A. Walz-Flannigan, J. R. Guest, and G. Raithel, Phys. Rev. Lett. **86**, 3993 (2001).
[22] F. Robicheaux, J. Phys. B **38**, S333 (2005).
[23] T. Killian, T. Pattard, T. Pohl, and J. Rost, Phys. Rep. **449**, 77 (2007).
[24] A. Griesmaier, J. Werner, S. Hensler, J. Stuhler, and T. Pfau, Phys. Rev. Lett. **94**, 160401 (2005).
[25] J. Stuhler, A. Griesmaier, T. Koch, M. Fattori, T. Pfau, S. Giovanazzi, P. Pedri, and L. Santos, Phys. Rev. Lett. **95**, 150406 (2005).
[26] J. M. Sage, S. Sainis, T. Bergeman, and D. DeMille, Phys. Rev. Lett. **94**, 203001 (2005).
[27] R. Barnett, D. Petrov, M. Lukin, and E. Demler, Phys. Rev. Lett. **96**, 190401 (2006).
[28] D. P. Fahey and M. W. Noel, Opt. Express **19**, 17002 (2011).
[29] F. Robicheaux, J. V. Hernández, T. Topcu, and L. D. Noordam, Phys. Rev. A **70**, 042703 (2004).
[30] S. Westermann, T. Amthor, A. L. de Oliveira, J. Deiglmayr, M. Reetz-Lamour, and M. Weidemüller, Eur. Phys. J. D **40**, 37 (2006).
[31] T. J. Carroll, C. Daniel, L. Hoover, T. Sidie, and M. W. Noel, Phys. Rev. A **80**, 052712 (2009).
[32] M. Viteau, A. Chotia, D. Comparat, D. A. Tate, T. F. Gallagher, and P. Pillet, Phys. Rev. A **78**, 040704 (2008).
[33] K. Afrousheh, P. Bohlouli-Zanjani, J. A. Petrus, and J. D. D. Martin, Phys. Rev. A **74**, 062712 (2006).
[34] T. Amthor, M. Reetz-Lamour, S. Westermann, J. Denskat, and M. Weidemüller, Phys. Rev. Lett. **98**, 023004 (2007).